Metacommunity-scale biodiversity regulation and the self-organized emergence of macroecological patterns

Running Title: Metacommunity-scale diversity regulation

Jacob D. O'Sullivan[1], Robert J. Knell[1], Axel G. Rossberg[1]

[1]School of Biological and Chemical Sciences, Queen Mary University of London, Mile End Road, London, E1 4NS, United Kingdom

Corresponding author: Jacob Dinner O'Sullivan, School of Biological and Chemical Sciences, Queen Mary University of London, Mile End Road, London E1 4NS, United Kingdom, (j.l.dinner@qmul.ac.uk, +447402090620)

Author contributions: AGR conceived of the study. JDO and AGR designed the model. JDO developed the model, performed simulations, analysed the data and drafted the manuscript. All three authors interpreted model outputs in comparison with observations and contributed to manuscript writing. The authors declare no competing interests.

Document statistics: Abstract - 150 words, main text - 4390 words, supporting information 277 words, citations - 73, main text figures - 6, supporting figures - 3

Keywords: biodiversity | macroecology | spatial ecology | metacommunity | ecological structural stability

Should this manuscript be accepted all simulation data supporting the results will be archived in a public repository and the data DOI will be included at the end of the article

Abstract

There exist a number of key macroecological patterns whose ubiquity suggests the spatio-temporal structure of ecological communities is governed by some universal mechanisms. The nature of these mechanisms, however, remains poorly understood. Here we probe spatio-temporal patterns species richness and community composition using a simple metacommunity assembly model. Despite making no *a priori* assumptions regarding biotic spatial structure or the distribution of biomass across species, model metacommunities self-organize to reproduce well documented patterns including characteristic species abundance distributions, range size distributions and species area relations. Also in agreement with observations, species richness in our model attains an equilibrium despite continuous species turnover. Crucially, it is in the neighbourhood of the equilibrium that we observe the emergence of these key macroecological patterns. Biodiversity equilibria in models occur due to the onset of ecological structural instability, a population-dynamical mechanism. This strongly suggests a causal link between local community processes and macroecological phenomena.

Introduction

Despite the colossal diversity of environments where life is found across the globe, there exist a number of spatio-temporal patterns in biodiversity which are observed in almost every ecological community that has been studied. The species abundance distribution (SAD), which highlights the overwhelming predominance of rare species in a given ecological community, has long been considered a universal phenomenon in ecology (Fisher et al., 1943; Preston, 1948). A related pattern, the range size distribution (RSD), points to the prevalence of small (Brown et al., 1996; Gaston, 1996), aggregated (Brown, 1984) ranges, with few species occupying broad distributions. The species area relation (SAR), which denontes the sub-linear increase in diversity as a function of sample area, has even achieved the privileged status of "one of community ecology's few genuine laws" (Schoener, 1976).

The less extensively studied (and considerably more divisive) phenomenon of community-level diversity regulation, which tends to constrain the number of species coexisting within an ecological assemblage, has also been proposed as a general ecological pattern (Gotelli et al., 2017; Magurran et al., 2018). The uniquely temporal signal of community regulation, which tends to produce robust levels of species richness despite continuous turnover in composition, makes detection challenging. Evidence of strong diversity regulation has, however, been found in desert rodents (Brown et al., 2000), birds (Parody et al., 2001), marine fish (Magurran et al., 2015), freshwater communities (Magurran et al., 2018), and in global-scale meta-analyses (Dornelas et al., 2014; Gotelli et al., 2017). At geological timescales, constrained diversification, assumed to reflect the impact of ecological limits on evolutionary processes, has been detected in the fossil record of a variety of taxa (Alroy, 2009, 2010; Liow and Finarelli, 2014; Benson et al., 2016). Indirect evidence of constrained diversification has been found in the rapid accumulation of diversity following mass extinction events (Krug and Patzkowsky, 2004; Brayard et al., 2009), and following major evolutionary innovations that increase the availability of ecological niches (Boyce et al., 2009; De Boer et al., 2012). Despite their apparent ubiquity, which strongly hints at some almost universal processes in macroecology, our mechanistic understanding of these spatio-temporal patterns in biodiversity remains disparate and incomplete.

The theory of island biogeography (MacArthur and Wilson, 1967) suggests that patterns in biodiversity may be explained as a consequence of the dependence of diversification rates – speciation, invasion and extinction – on standing diversity. In island systems, diversity regulation emerges as the rate of accumulation of new species converges on the rate of species loss, both of which are strongly dependent on the size of the existing species pool. In the fifty years since the Theory of Island Biogeography was first developed, however, the effects of environmental heterogeneity, landscape topography, local species interactions and dispersal have been shown to impact local and regional diversity patterns in complex ways (Shmida and Wilson, 1985; Holt, 1985; Pulliam, 1988). Contemporary metacommunity ecology (Leibold et al., 2004; Holyoak et al., 2005; Logue et al., 2011; Winegardner et al., 2012) shines a light on how these complex and overlapping processes interact. Perhaps due to the persistent

view that local and regional ecological processes cannot be meaningfully unified (Harmon and Harrison, 2015), surprisingly few studies consider metacommunity frameworks that explicitly incorporate community dynamics at multiple spatial scales (e.g. Pillai et al., 2010; Barter and Gross, 2017; but see Plitzko and Drossel, 2015; Thiel and Drossel, 2018). Here we attempt to fill this gap with a dynamically simple metacommunity assembly model which accounts for local ecological interactions and dispersal in an environmentally heterogeneous landscape, thus uniting the branches of population-dynamical and spatial ecology. Our primary focus in developing this model was the study of how biodiversity might be regulated in spatially resolved ecological assemblages, but we find an intriguing emergent relationship between diversity regulation in model metacommunities and the appearance of widely observed macroecological patterns.

In spatially *unresolved* models, the emergence of biodiversity regulation has been observed numerous times (e.g. Drossel et al., 2001; Yoshida, 2003; Pawar, 2009). It can been shown analytically (Rossberg, 2013) that the loss of *ecological structural stability*, which denotes the robustness of assemblages to press (i.e. sustained) perturbations (Meszéna et al., 2006; Bastolla et al., 2009; Rossberg, 2013; Rohr et al., 2014), is the mechanism driving this diversity dependent diversification in such simple models. A strongly regulated community is one that has converged on its *structurally unstable* diversity limit, determined by the intensity of ecological interactions within that community (Rossberg, 2013). In order to understand the relationship between diversity regulation, via the onset of ecological structural instability, and the processes active in metacommunities, we developed a multi-species framework in which metapopulation dynamics at the regional scale are modelled using a spatial network of Lotka-Volterra competition equations of the basic form

$$\frac{db_i}{dt} = \left(r_i - \sum_j^S \mathbf{A}_{ij} b_j \right) b_i \qquad (1 \leq i \leq S), \tag{1}$$

with b_i denoting population biomass, r_i linear growth rate, $\mathbf{A}_{ij}$ interaction strength, and S species richness, that are coupled through additional terms describing dispersal (see *Dynamic equations and metacommunity assembly*, below).

By comparing the model's behaviour to analytic predictions developed for spatially unresolved competitive communities (Rossberg, 2013), we show, for the first time, that intrinsic metacommunity-level diversity regulation can indeed be explained as a consequence of the onset ecological structural instability at the *regional* scale. Surprisingly, and potentially very importantly, we find that, as model metacommunities approach diversity limits, they *self organize* to reproduce the macroecological patterns previously identified as central for the spatial structure of biodiversity (McGill, 2010): a skewed local and regional distribution of abundances, spatial aggregation of conspecific biomass, and apparent absence of species co-occurrence patterns. In combination, as McGill (2010) argued, these core patterns lead to sub-linear species area relations and other spatial biodiversity phenomena. That a diverse set of well known macroecological patterns emerges in a simple metacommunity model—describing nothing but dispersal of locally interacting species—strongly supports the hypothesis that these patterns are indeed indirect consequences

of local population dynamics and dispersal. Furthermore, this study adds to the growing body of evidence which suggests ecological structural stability may represent a key organising principle in natural communities (Rossberg, 2013; Rossberg et al., 2017).

Results and discussion

Metacommunity species richness

Simulated metacommunities, assembled in our model via a constant, slow influx of invaders, converge on regional diversity equilibria at which species richness remains approximately stationary despite continuous turnover in the species composition (Fig. 1). Diversity relaxes back to the same approximate steady state after major disturbances, modelled as a sudden removal or introduction of large numbers of species (Fig. 1).

From previous theoretical work we know that the sensitivity of a spatially unresolved community to press perturbations is a function of the standing diversity and the intensity of ecological interactions within that community (Rossberg, 2013). The structurally unstable limit around which diversity in model communities converges, denoted S^*, is a function of the statistical distribution in competition coefficients. By assuming a precisely analogous mechanism to operate at the metacommunity scale, this spatially unresolved theory predicts an approximate *regional* diversity of

$$S^* = \frac{\left(1 - \mathsf{E}[\mathbf{C}_{ij}]\right)^2}{2\,\mathrm{var}\,(\mathbf{C}_{ij})} \qquad (i \neq j), \tag{2}$$

where $\mathsf{E}[\mathbf{C}_{ij}]$ and $\mathrm{var}\,(\mathbf{C}_{ij})$ represent the expectation and variance of the coefficients of interspecific competition computed at the scale of the metacommunity, replacing the distribution of local interaction coefficients $\mathbf{A}_{ij}$ in the spatially unresolved theory. The eigenvalue spectrum of the competitive overlap matrix also offers a convenient graphical tool for assessing the ecological structural instability of a model community. The structurally unstable diversity limit occurs as the area covered by the spectrum in the complex plane approach the origin (Rossberg, 2013).

Regional-scale, interspecific competition coefficients $\mathbf{C}_{ij}$ were computed for model metacommunities assembled with a for range of parameter combinations, and used to evaluate Eq. 2 (see *Regional scale interaction matrices* below). Comparing the diversity predicted by Eq. 2 with that in the steady state of the simulation, we found that the spatially unresolved analytic prediction explains 95% of variance in the equilibrium species richness in the spatially resolved models (Fig. 2A). Furthermore, the spectra of the matrices $\mathbf{C}$ approach the origin when the biodiversity equilibrium is reached (Fig. 2B), just as observed in spatially unresolved models (Rossberg, 2013). Thus, although an analytic prediction of the structurally unstable diversity limit

in the metacommunity case is not available due to the intractability of the full model, we find strong evidence to support the claim that ecological structural stability drives diversity regulation at the metacommunity scale.

The relationship between local on regional competition coefficients is non-trivial; it depends, among others, on the degree of spatial heterogeneity (see *Model landscape*, below). Nonetheless, we found the off-diagonal elements of $\mathbf{A}_{ij}$ and $\mathbf{C}_{ij}$ to be significantly correlated in metacommunity models at regional diversity limits ($p < 0.01$, for all parameter combinations). This implies that, though the impact of environmental heterogeneity on realised regional-scale competition is complex, local ecological interactions do indeed propagate to the metacommunity scale and influence regional diversity patterns. Thus, our model metacommunities conform with the Ecological Limits Hypothesis (Rabosky and Hurlbert, 2015), according to which ecological factors associated with resource partitioning determine species richness at large spatial scales. For further discussion see Supporting Information.

Local species richness

In order to distinguish between local and regional diversity it is necessary to define some criterion for assessing presence-absence in a local assemblage. We do this in two ways. First by setting an arbitrary limit, equivalent to a detection threshold, of 10^{-4} biomass units below which a species is considered to be absent from a local community. This value is four orders of magnitude less that the maximum local biomass permitted in the model and therefore defines a detectable range that is in accordance with many empirical observations (e.g. Condit et al., 2002). We then distinguish further among those populations exceeding the detection threshold by defining *source* and *sink* populations as, respectively, those capable of self maintenance in a given location, and those that would decline without continuous immigration from adjacent communities (see *Source-Sink classification*, below). A comparable criterion has been applied to populations in an esturine fish community to distinguish between 'core' species, temporally persistent and well adapted to local conditions, and 'occasional' species, which are infrequently observed, poorly adapted and accordingly of typically low abundance (Magurran and Henderson, 2003).

During the assembly process (Fig. 1), we find that local community richness, defined by the detection threshold, saturates earlier than the regional assemblage (after around $\sim$ 500 and $\sim$ 4000 invasions, respectively, in the example shown). To confirm whether this local community regulation occurs independently of metacommunity regulation, it is necessary to ask how α-diversity is related to γ-diversity. If local diversity limits are controlled indirectly by the size of the regional species pool (i.e. regulation occurs meaningfully at one scale only) we would expect a linear, or at least non-saturating local-regional species richness relation. Interestingly, however, both source and sink diversity, and, by extension, their sum, are saturating functions of the regional species richness in equilibrium metacommunities. As we show in Fig. 3A, for which the distribution of interspecific coefficients $\mathbf{A}_{ij}$ was fixed across simulations, average local diversity of source populations converged on a horizontal asymptote

of ~ 50 once the regional assemblage reached ~ 300 species. Similar convergence, though with greater scatter, is evident for sink populations, though the asymptote may occur outside of the range studied here. This shows that local diversity is indeed independently regulated, such that in sufficiently large regional communities local diversity is effectively independent of the metacommunity-scale parameterization that determines the size of the regional species pool. A comparable degree of saturation in the local-regional richness ratio (sub-linear on double-log axes, not shown) has been observed, for example, in tropical reef building coral communities (Karlson and Cornell, 2002).

To understand whether regulation at local scales also occurs due to the onset of structural instability, we determined, for any given site, the sub-matrix of $\mathbf{A}$ corresponding to the local source population. We found that the spectra of these sub-matrices, too, approach the origin of the complex plane. This is evidence that structural instability regulates species richness not only at the metacommunity level, but independently also at the local level (Fig. 3B).

Temporal turnover

Stationarity in species richness is a key and unambiguous characteristic of our model metacommunities. Less obvious is the fact that, rather than converging on a near-static, 'climax' community, regional scale composition in our models continuously turns over in response to the slow flux of invaders (Fig. 4A). Interestingly, on average, local communities turn over faster than the regional metacommunity of which they form a part. This is seen in the rapid decay in community similarity at the local, relative to the regional scale (Fig. 4A). The independent diversity regulation at the local scale, which implies to high sensitivity of local communities to changes in the species composition of their neighbourhood, might contribute to this fast local turnover. If the invader flux is spontaneously stopped and instead species are experimentally removed from the regional community in increasing order of regional biomass, fast turnover at local scales buffers local communities from diversity losses at the metacommunity scale (Fig. 4B). In the example shown in Fig. 4, a 20% decrease in regional species richness produced only a 13% drop at the local scale on average. It has been estimated that the current rate of global species loss is 100-1000 times the background rate (De Vos et al., 2015; Pimm et al., 2014; Ceballos et al., 2015), yet global meta-analyses have failed to detect a consistent loss of diversity at the local scale (Dornelas et al., 2014; Vellend et al., 2017; Gotelli et al., 2017). Our results suggest that differences in relaxation time due to regulatory processes at multiple spatial scales may account for the discrepancy between local and regional/global diversity trends.

Spatial patterns in biodiversity and abundance

By elegantly comparing the various major efforts to devise unified macroecological theory to date, McGill (2010) showed that three key macoecological phenomena are basic assumptions implicit to all frameworks. McGill argued that these key phenomena

on their own are sufficient to give rise to a variety of emergent macroecological patterns, such as the sub-linear SAR. The three key patterns include an uneven SAD at various spatial scales, the spatial aggregation of conspecific biomass underlying the observed skewed RSD, and the (apparent) non-signficant correlation in species' spatial distributions. The last phenomenon relates to the observation that statistically significant positive or negative correlations in species' spatial distributions or co-occurrence patterns are surprisingly under-represented in empirical studies; most pair-wise correlations tend to be indistinguishable from random (Hoagland and Collins, 1997; Veech, 2006; Houlahan et al., 2007; D'Amen et al., 2018). We find that, surprisingly, each of these three patterns emerges in our model metacommunities in the neighbourhood of regional diversity equilibria (Fig. 5).

Figure 5A shows that at both local and regional scale the SAD conforms to the left-skewed log-normal paradigm, observed in communities ranging from marine benthos to Amazonian rain forest (McGill et al., 2007). The early onset of diversity regulation at the local scale already leads to highly skewed SAD at the regional scale, after which further accumulation of diversity at the regional scale drives the distribution to the left as average biomasses decline.

In the early stages of the assembly process, as local diversity accumulates, weak biotic filtering means species disperse across much of their fundamental geographic niche. Once local limits to diversity become relevant, regional scale invasions instead drive an increase in spatial β-diversity, achieved by a reduction of species ranges, which become highly spatially aggregated (Fig. S2). At the metacommunity scale this corresponds to a collapse in the RSD as the assemblage approaches regional diversity equilibrium (Fig. 5B). The skewed model RSD for metacommunities at the regional diversity limit match the pattern observed for a wide variety of taxa (Gaston, 1998), including pine species (Brown et al., 1996), tropical tree species (Xu et al., 2015) and in both regional (Gaston, 1996), and global distributions (Orme et al., 2006) of bird species.

The dependence of range sizes on species richness implies a strong impact of ecological interactions on species' realised ranges in models. Counter-intuitively, however, the vast majority of species pairs show no significant spatial correlation (Fig. 5C). As strong regional scale diversity regulation sets in and metapopulation ranges collapse, the percentage of species pairs for which it is possible to detect non-random spatial correlation drops to near zero, giving the impression of an eminently neutral system.

We considered the possibility that this absence of demonstrable spatial correlations is explained by the systemic exclusion of competing species pairs during assembly. However, for fully assembled model metacommunities at the regional diversity limit, non-zero interspecific competition coefficients made up 21.5–28.3% of the elements of the matrix $\mathbf{A}_{ij}$, only 1.7–8.5% less than in the statistical ensemble from which invaders are sampled. This is insufficient to explain the observed absence of spatial correlation.

McGill (2010) argues that these three key phenomena (Fig. 5) can combine to produce sub-linearity in the SAR. A recent non-dynamical modelling approach has verified that spatial aggregation at the population scale can indeed generate high level

macroecological configurations (Takashina et al., 2018). Here we build on that result by showing that population-dynamical processes can drive spatial aggregation and, as a result, produce the characteristic relationship between diversity and landscape area. The SAR in our models (Fig. 6) are well approximated by power laws with exponents ranging from 0.19 to 0.87, depending on the degree of spatial correlation in the model environment: a spatially more correlated, homogeneous environment produces an SAR with lower exponent. The exponents are well within the range found in a meta-analysis of almost 800 empirical SARs (Drakare et al., 2006).

Conclusions

There is a growing body of evidence indicating that community level diversity regulation is a common characteristic of ecological communities at both local and regional scales (e.g. Alroy, 2009; Magurran et al., 2015, 2018; Gotelli et al., 2017; Dornelas et al., 2014). Proponents of this equilibrial paradigm concede that a precise mechanism explaining community regulation remains elusive (Magurran et al., 2018). Here we show for the first time that ecological structural instability can drive diversity regulation at multiple spatial scales in model metacommunities, offering a potential resolution to this problem.

With this model we set out to assess the degree to which spatially unresolved ecological theory can incorporate the complex spatial processes occurring within a model metacommunity. To our surprise, metacommunity models which explicitly incorporate dynamics at both local and regional scales reproduce an unprecedented range of empirically ubiquitous macroecological patterns. Our models reproduce temporal patterns in species richness and community composition, left-skewed log-normal SAD at multiple spatial scales, spatial aggregation and a skewed RSD, power-law SAR, as well as more nuanced patterns like the local-regional richness relations. Crucially, these patterns result indirectly from the local dynamics, and in the neighbourhood of regional diversity limits. From this observation we conclude that there is an important interaction between the system-scale dynamical process central to the theory of ecological structural stability, and these key macroecological configurations.

If we conclude, on the basis of this and similar studies, that diversity regulation is indeed a common or general feature of ecological communities, this would entail a paradigm shift with important implications for the conservation and management of biodiversity. Our model tells us that local biotic interactions can determine the diversity occurring at the regional scale (Rabosky and Hurlbert, 2015). The fact that many species occupy non-overlapping ranges does not mean that biotic interactions are of little importance (Harmon and Harrison, 2015). Spatial segregation due to local biotic and abiotic filtering weakens ecological interactions (Fig. S3), thus permitting more species to coexist regionally than in a single local community, but regulation of regional diversity is, nevertheless, controlled by these interactions (Fig. 2).

The assumption that ecological interactions have negligible impact on regional biotic distributions is still implicit in the

majority of current conservation policies and programs. Species distribution modelling (SDM) is a widely used method for identifying ecological processes and responses of species distributions to environmental change. The basic SDM methodology assumes a comprehensive understanding of current and future climate is sufficient to predict range shifts under climate change. Our results suggest that abandoning biotic interactions, even if they cannot be explicitly detected using conventional tools, may strongly undermine the effectiveness of these models (Wisz et al., 2013). As such, we suggest that the development and application of more mechanistic distribution modelling (Dormann et al., 2018) should be a priority, that management models might focus on higher levels of biological organisation (e.g. feeding guilds or entire communities), and that designers of conservation and management strategies make a concerted effort to integrate factors relating to diversity regulation in their decision making.

Methods

Model landscape

We generated a spatial network consisting of N patches by sampling the Cartesian coordinates (P_x, Q_x) of each patch x (with $1 \leq x \leq N$) from a uniform distribution in the range $(0, \sqrt{N})$. The patches, or local communities, were thus randomly distributed with density ≈ 1 over a model landscape of area N. Corridors (edges) were added to the network (graph) using to the Gabriel algorithm (1969) (Fig. S2), which ensures that in the limit of large N the average patch degree does not exceed 4 (Matula and Sokal, 1980).

Environmental heterogeneity was modelled indirectly through spatial variation in species' linear growth rates r_{ix}, where the subscript i is a species index, and x a patch index. The values of r_{ix} were sampled from a Gaussian Random Field (Adler, 1981) ($\mu = 1.0$, $\sigma^2 = 0.5$), generated via eigen-decomposition of the covariance matrix (Johnson and Wichern, 2002), with exponentially decaying spatial correlations of characteristic length ϕ. With d_{xy} denoting the Euclidean distances between two patches x and y, the correlation between random r_{ix} and r_{iy} is $\exp\left[-\phi^{-1} d_{xy}\right]$ for and any species i. By varying the correlation length ϕ while keeping mean and variance of the fields fixed, we modelled landscapes of varying degrees of environmental heterogeneity. Parameters were chosen as $N = 10$, $\phi = 1$ for Fig. 1, $N = 20$, $\phi = 1$ for Figs. 4, and 5. (Temporal decoupling of spatial scales is clearer in larger regional communities, however for γ-diversity $\gg$ α-diversity it becomes difficult to represent local and regional assemblages on a single axis.) Figs. 2, 3, and 6 summarize the complete parameter space studied: $N = 2$, 4, 6, 8, 10, 12, 15, 20, and 25; $\phi = 1$, 2, 5, 10, 20, 40, 80, and 160, in all combinations.

Dynamic equations and metacommunity assembly

We used a spatial extension of the Lotka-Volterra multi-species competition equation to model local population dynamics and dispersal in our model metacommunities, thus building on the model family pioneered by Reichenbach et al. (2007). The rate of change of local biomass of species i at patch x is given by the non-linear ordinary differential equation

$$\begin{aligned}\frac{db_{ix}}{dt} = & b_{ix}\left(r_{ix} - \sum_{j=1}^{S} \mathbf{A}_{ij}\, b_{jx}\right) - e\, b_{ix} \\ & + \sum_{y \in \mathcal{N}(x)} \frac{e}{k_y} \exp\left(-d_{xy}\ell^{-1}\right)\, b_{iy}.\end{aligned} \tag{3}$$

The system of $N \times S$ coupled equations can therefore be written as

$$\frac{d\mathbf{B}}{dt} = \mathbf{B} \circ (\mathbf{R} - \mathbf{A}\mathbf{B}) + \mathbf{B}\mathbf{D}, \tag{4}$$

with $\circ$ denoting element-wise multiplication.

The first term on the right hand side of Eq. 3 represents the local dynamics, where $\mathbf{A}_{ij}$ are the entries of the spatially unresolved competitive overlap matrix. In simulations, the off-diagonal entries $\mathbf{A}_{ij}$ were sampled randomly, with $\mathbf{A}_{ij}$ set to 0.3 with probability 0.3 and to 0 otherwise. The diagonal entries, representing intraspecific competition, were always set to 1. The second term on the right of Eq. 3 represents the rate at which biomass of species i emigrates away from patch x, while the third term gives the immigration rates from all patches y sharing an edge with x. The immigration rate decays exponentially with characteristic length ℓ, kept fixed at 0.2. The parameter e, which represents the fraction of biomass leaving patch x per unit time, is kept fixed at 0.02. The normalization constant k_y divides the biomass departing patches y between all other patches in the *its* local neighbourhood ($\mathcal{N}(y)$), weighted by the ease of reaching each patch i.e. $k_y = \sum_{z \in \mathcal{N}(y)} \exp\left(-d_{yz}\ell^{-1}\right)$. Further investigation of the effect of varying the nature and strength of dispersal processes in model metacommunities will be the focus of future work.

We adopted the community assembly modelling approach first developed by Post and Pimm (1983). In each iteration of the algorithm, a new species was added to the metacommunity. Invaders were selected by computing the linear growth rate at low abundance of new species i with randomly generated ecologies (r_{ix} and $\mathbf{A}_{ij}$), until a species with positive linear growth rate was found. This was then added to a randomly selected patch with a fixed, low invasion biomass of 0.01 times the detection threshold of 10^{-4} biomass units. The metacommunity dynamics were then simulated using the SUNDIALS numerical ODE solver (Hindmarsh et al., 2005) over 500 unit times, t. Those species whose biomass dropped below the detection threshold

in all patches of the network were considered regionally extinct and removed from the system. By thus iteratively adding species to the community we modelled a constant flux of invaders, which causes the regional assemblage to turn over and self-organize, eventually converging on an equilibrium at which the average extinction rate balances the invasion rate. To reach this equilibrium, total simulation time was chosen as 4000, 6000, 8000, 10000, and 12000 iterations for $N \leq 4$, $6 \leq N \leq 10$, $12 \leq N \leq 15$, $N = 20$ and $N = 25$, respectively.

Source-Sink classification

Source populations in a given patch x are those capable of locally maintaining themselves. Mathematically, a population b_{ix} was defined as a source population when its local biomass was greater than the detection threshold and $r_{ix} - \sum_{j=1}^{S} \mathbf{A}_{ij} b_{jx} \geq 0$. Conversely, it was defined as a sink populations when its local biomass was greater than the detection threshold and $r_{ix} - \sum_{j=1}^{S} \mathbf{A}_{ij} b_{jx} < 0$.

Regional scale interaction matrices

In order to compare model metacommunity dynamics to theoretical predictions, we numerically computed a spatially unresolved competitive overlap matrix that describes dynamics at the regional scale. For this we constructed a spatially *unresolved* Lotka-Volterra system,

$$d\mathsf{B}_i/dt = (\rho_i - \sum_{j=1}^{S} \hat{\mathbf{C}}_{ij} \mathsf{B}_i) \cdot \mathsf{B}_i, \tag{5}$$

where B_i represents total biomass of species i, as an approximation of the spatially *resolved* model (Eq. 3). This required integrating ecological interactions over the entire computational landscape, which was done using the computational equivalent of a harvesting experiment. We asked how the steady state community responds to spatially independent harvesting of a single species, and determined the coefficients $\hat{\mathbf{C}}_{ij}$ of the unresolved model accordingly.

For the unresolved case the harvesting of species i at a rate h, modelled by substituting $\rho_i - h$ for ρ_i in Eq. 5, produces a shift in the equilibrium biomasses given by

$$\Delta \mathsf{B}_j = -\hat{\mathbf{C}}_{ij}^{-1} h. \tag{6}$$

The most computationally efficient way of conducting the corresponding experiment for the meta-community is to use a numerical approximation of the Jacobian matrix. In doing so, we assume simulated metacommunities to be at fixed points, an approximation that is justified retrospectively by the apparently efficacy of the method. The elements of the Jacobian are given

by the general equation

$$\mathbf{J}_{ixjy} = \frac{\partial f_{ix}(b_{11}, \ldots, b_{S1}, \ldots, b_{1N}, \ldots b_{SN})}{\partial b_{jy}}, \tag{7}$$

evaluated at equilibrium. The functions f_{ix} denote the right hand side of Eq. 3.

Light harvesting of a single focal species i at a rate h brings about a small shift in the equilibrium biomasses of the other species in the metacommunity and the dynamics of the harvested community *near the unharvested equilibrium* (b^*_{jy}) can be approximated by

$$\frac{db_{ix}}{dt} = \left(\sum_{jy} \mathbf{J}_{ixjy}(b_{jy} - b^*_{jy})\right) - hb_{ix}, \quad \text{and} \tag{8a}$$

$$\frac{db_{kx}}{dt} = \left(\sum_{jy} \mathbf{J}_{kxjy}(b_{jy} - b^*_{jy})\right) \quad \text{for } k \neq i\ . \tag{8b}$$

Here h is the harvesting rate. We vectorize the matrix $\mathbf{B}$ (denoted $\vec{\mathbf{B}}$) in order to match the dimensionality of the spatially resolved Jacobian, and the write the equilibrium condition for Eq. 8a as

$$\mathbf{J}(\vec{\mathbf{B}} - \vec{\mathbf{B}}^*) - \vec{\mathbf{H}} = 0, \tag{9}$$

where the elements of vector $\vec{\mathbf{H}}$ are hb_{jy} for $j = i$ and 0 otherwise. From this, we obtain

$$h^{-1}\left(\vec{\mathbf{B}} - \vec{\mathbf{B}}^*\right) = \mathbf{J}^{-1}h^{-1}\vec{\mathbf{H}}. \tag{10}$$

The left hand side of Eq. 10 represents the local shift in biomasses due to the harvesting of the focal species i per unit h. From Eq. 10 we compute the change in total biomass $\Delta \mathsf{B}_j$ of each species j. Comparison with 6 gives row i of $\hat{\mathbf{C}}^{-1}$. Iterating over all species $i = 1 \ldots S$, we computed $\hat{\mathbf{C}}^{-1}$and from this the spatially unresolved interaction matrix $\hat{\mathbf{C}}$. Finally, in order to match the assumptions made in the derivation of Eq. 2 (Rossberg, 2013), we divided each row and column $\hat{\mathbf{C}}$ by the square root of the corresponding diagonal element to obtain the *effective competitive overlap matrix*, $\mathbf{C}$ (which has ones along the diagonal).

Temporal diversity patterns

Temporal species richness and turnover in community composition were computed for a metacommunity at regional diversity limits for a period corresponding to 500 ecological invasions (Fig. 4). Species richness analysis requires the application of some presence-absence criterion. We assess local community diversity by reference to the source populations only, since sink populations are effectively decoupled from local filtering processes by dispersal.

Following the 500 invasions, species were removed in reverse order of regional abundance, in order to model a large scale mass extinction process. A single metacommunity of $N = 20$, $\phi = 2$ was used for this analysis.

Community turnover (Fig. 4A) was measured using the Bray-Curtis (1957) similarity index computed using the function **vegdist** in the R package "vegan" (Oksanen et al., 2018).

Species ranges

In order to quantify range sizes of species, we first computed, for each species, the covariance matrix

$$\Sigma = \begin{pmatrix} \mathrm{var}(P_x) & \mathrm{cov}(P_x, Q_x) \\ \mathrm{cov}(P_x, Q_x) & \mathrm{var}(Q_x) \end{pmatrix} \tag{11}$$

of the locations (P_x, Q_x) of individuals forming the species' population, assuming population sizes are proportional to biomasses at each patch. Thus, $\mathrm{var}(P_x)$ is, for example, the variance of the of the biomass distribution of the population of the focal species along the P axis. As a measure of range size, we then computed the product of the square roots of the eigenvalues of Σ, i.e. the square root of its determinant, $\sqrt{\det|\Sigma|}$. By this measure, an even distribution of biomass over the full $\sqrt{N} \times \sqrt{N}$ rectangle enclosing one of our model communities corresponds to a range size of $N/12$.

Species co-occurrence

In order to analyse the correlation in species spatial distributions within our model landscapes, we used the probabilistic model developed by Veech (2013) included in the R package "cooccur" (Griffith et al., 2016), which compares observed pair-wise co-occurrence to that expected if two species were distributed independently within a discretized landscape.

References

R. J. Adler. *The geometry of random fields*, volume 62. Siam, 1981.

J. Alroy. Speciation and extinction in the fossil record of north american mammals. In R. Butlin, J. Bridle, and D. Schluter, editors, *Speciation and patterns of diversity*, chapter 16. Cambridge University Press, 2009.

J. Alroy. Geographical, environmental and intrinsic biotic controls on phanerozoic marine diversification. *Palaeontology*, 53(6): 1211–1235, 2010.

E. Barter and T. Gross. Spatial effects in meta-foodwebs. *Scientific Reports*, 7(1):9980, 2017.

U. Bastolla, M. A. Fortuna, A. Pascual-García, A. Ferrera, B. Luque, and J. Bascompte. The architecture of mutualistic networks minimizes competition and increases biodiversity. *Nature*, 458(7241):1018, 2009.

R. B. Benson, R. J. Butler, J. Alroy, P. D. Mannion, M. T. Carrano, and G. T. Lloyd. Near-stasis in the long-term diversification of mesozoic tetrapods. *PLoS biology*, 14(1):e1002359, 2016.

C. K. Boyce, T. J. Brodribb, T. S. Feild, and M. A. Zwieniecki. Angiosperm leaf vein evolution was physiologically and environmentally transformative. *Proceedings of the Royal Society of London B: Biological Sciences*, 276(1663):1771–1776, 2009.

J. R. Bray and J. T. Curtis. An ordination of the upland forest communities of southern wisconsin. *Ecological monographs*, 27 (4):325–349, 1957.

A. Brayard, G. Escarguel, H. Bucher, C. Monnet, T. Brühwiler, N. Goudemand, T. Galfetti, and J. Guex. Good genes and good luck: ammonoid diversity and the end-permian mass extinction. *Science*, 325(5944):1118–1121, 2009.

J. H. Brown. On the relationship between abundance and distribution of species. *The american naturalist*, 124(2):255–279, 1984.

J. H. Brown, G. C. Stevens, and D. M. Kaufman. The geographic range: size, shape, boundaries, and internal structure. *Annual review of ecology and systematics*, 27(1):597–623, 1996.

J. H. Brown, S. M. Ernest, J. M. Parody, and J. P. Haskell. Regulation of diversity: maintenance of species richness in changing environments. *Oecologia*, 126(3):321–332, 2000.

G. Ceballos, P. R. Ehrlich, A. D. Barnosky, A. García, R. M. Pringle, and T. M. Palmer. Accelerated modern human–induced species losses: Entering the sixth mass extinction. *Science advances*, 1(5):e1400253, 2015.

R. Condit, N. Pitman, E. G. Leigh, J. Chave, J. Terborgh, R. B. Foster, P. Núnez, S. Aguilar, R. Valencia, G. Villa, et al. Beta-diversity in tropical forest trees. *Science*, 295(5555):666–669, 2002.

M. D'Amen, H. K. Mod, N. J. Gotelli, and A. Guisan. Disentangling biotic interactions, environmental filters, and dispersal limitation as drivers of species co-occurrence. *Ecography*, 41(8):1233–1244, 2018.

H. J. De Boer, M. B. Eppinga, M. J. Wassen, and S. C. Dekker. A critical transition in leaf evolution facilitated the cretaceous angiosperm revolution. *Nature Communications*, 3:1221, 2012.

J. M. De Vos, L. N. Joppa, J. L. Gittleman, P. R. Stephens, and S. L. Pimm. Estimating the normal background rate of species extinction. *Conservation Biology*, 29(2):452–462, 2015.

C. F. Dormann, M. Bobrowski, D. M. Dehling, D. J. Harris, F. Hartig, H. Lischke, M. D. Moretti, J. Pagel, S. Pinkert, M. Schleuning, et al. Biotic interactions in species distribution modelling: 10 questions to guide interpretation and avoid false conclusions. *Global Ecology and Biogeography*, 2018.

M. Dornelas, N. J. Gotelli, B. McGill, H. Shimadzu, F. Moyes, C. Sievers, and A. E. Magurran. Assemblage time series reveal biodiversity change but not systematic loss. *Science*, 344(6181):296–299, 2014.

S. Drakare, J. J. Lennon, and H. Hillebrand. The imprint of the geographical, evolutionary and ecological context on species–area relationships. *Ecology letters*, 9(2):215–227, 2006.

B. Drossel, P. G. Higgs, and A. J. McKane. The influence of predator–prey population dynamics on the long-term evolution of food web structure. *Journal of Theoretical Biology*, 208(1):91–107, 2001.

R. A. Fisher, A. S. Corbet, and C. B. Williams. The relation between the number of species and the number of individuals in a random sample of an animal population. *The Journal of Animal Ecology*, pages 42–58, 1943.

K. R. Gabriel and R. R. Sokal. A new statistical approach to geographic variation analysis. *Systematic zoology*, 18(3):259–278, 1969.

K. J. Gaston. Species-range-size distributions: patterns, mechanisms and implications. *Trends in Ecology & Evolution*, 11(5): 197–201, 1996.

K. J. Gaston. Species-range size distributions: products of speciation, extinction and transformation. *Philosophical Transactions of the Royal Society B: Biological Sciences*, 353(1366):219–230, 1998.

N. J. Gotelli, H. Shimadzu, M. Dornelas, B. McGill, F. Moyes, and A. E. Magurran. Community-level regulation of temporal trends in biodiversity. *Science advances*, 3(7):e1700315, 2017.

D. M. Griffith, J. A. Veech, C. J. Marsh, et al. cooccur: Probabilistic species co-occurrence analysis in r. *J Stat Softw*, 69(2): 1–17, 2016.

L. J. Harmon and S. Harrison. Species diversity is dynamic and unbounded at local and continental scales. *The American Naturalist*, 185(5):584–593, 2015.

A. C. Hindmarsh, P. N. Brown, K. E. Grant, S. L. Lee, R. Serban, D. E. Shumaker, and C. S. Woodward. Sundials: Suite of nonlinear and differential/algebraic equation solvers. *ACM Transactions on Mathematical Software (TOMS)*, 31(3):363–396, 2005.

B. W. Hoagland and S. L. Collins. Gradient models, gradient analysis, and hierarchical structure in plant communities. *Oikos*, pages 23–30, 1997.

R. D. Holt. Population dynamics in two-patch environments: some anomalous consequences of an optimal habitat distribution. *Theoretical population biology*, 28(2):181–208, 1985.

M. Holyoak, M. A. Leibold, and R. D. Holt. *Metacommunities: spatial dynamics and ecological communities*. University of Chicago Press, 2005.

J. E. Houlahan, D. J. Currie, K. Cottenie, G. S. Cumming, S. Ernest, C. S. Findlay, S. D. Fuhlendorf, U. Gaedke, P. Legendre, J. J. Magnuson, et al. Compensatory dynamics are rare in natural ecological communities. *Proceedings of the National Academy of Sciences*, 104(9):3273–3277, 2007.

R. A. Johnson and D. Wichern. *Multivariate analysis*. Wiley Online Library, 2002.

R. H. Karlson and H. V. Cornell. Species richness of coral assemblages: detecting regional influences at local spatial scales. *Ecology*, 83(2):452–463, 2002.

A. Krug and M. Patzkowsky. Rapid recovery from the late ordovician mass extinction. *Proceedings of the National Academy of Sciences of the United States of America*, 101(51):17605–17610, 2004.

M. A. Leibold, M. Holyoak, N. Mouquet, P. Amarasekare, J. M. Chase, M. F. Hoopes, R. D. Holt, J. B. Shurin, R. Law, D. Tilman, et al. The metacommunity concept: a framework for multi-scale community ecology. *Ecology letters*, 7(7): 601–613, 2004.

L. H. Liow and J. A. Finarelli. A dynamic global equilibrium in carnivoran diversification over 20 million years. In *Proc. R. Soc. B*, volume 281. The Royal Society, 2014.

J. B. Logue, N. Mouquet, H. Peter, H. Hillebrand, M. W. Group, et al. Empirical approaches to metacommunities: a review and comparison with theory. *Trends in ecology & evolution*, 26(9):482–491, 2011.

R. H. MacArthur and E. O. Wilson. The theory of island biogeography. *Princeton, NJ*, 1967.

A. E. Magurran and P. A. Henderson. Explaining the excess of rare species in natural species abundance distributions. *Nature*, 422(6933):714, 2003.

A. E. Magurran, M. Dornelas, F. Moyes, N. J. Gotelli, and B. McGill. Rapid biotic homogenization of marine fish assemblages. *Nature communications*, 6:8405, 2015.

A. E. Magurran, A. E. Deacon, F. Moyes, H. Shimadzu, M. Dornelas, D. A. Phillip, and I. W. Ramnarine. Divergent biodiversity change within ecosystems. *Proceedings of the National Academy of Sciences*, page 201712594, 2018.

D. W. Matula and R. R. Sokal. Properties of gabriel graphs relevant to geographic variation research and the clustering of points in the plane. *Geographical analysis*, 12(3):205–222, 1980.

B. J. McGill. Towards a unification of unified theories of biodiversity. *Ecology letters*, 13(5):627–642, 2010.

B. J. McGill, R. S. Etienne, J. S. Gray, D. Alonso, M. J. Anderson, H. K. Benecha, M. Dornelas, B. J. Enquist, J. L. Green, F. He, et al. Species abundance distributions: moving beyond single prediction theories to integration within an ecological framework. *Ecology letters*, 10(10):995–1015, 2007.

G. Meszéna, M. Gyllenberg, L. Pásztor, and J. A. Metz. Competitive exclusion and limiting similarity: a unified theory. *Theoretical Population Biology*, 69(1):68–87, 2006.

J. Oksanen, F. G. Blanchet, M. Friendly, R. Kindt, P. Legendre, D. McGlinn, P. R. Minchin, R. B. O'Hara, G. L. Simpson, P. Solymos, M. H. H. Stevens, E. Szoecs, and H. Wagner. *vegan: Community Ecology Package*, 2018. URL `https://CRAN.R-project.org/package=vegan`. R package version 2.4-6.

C. D. L. Orme, R. G. Davies, V. A. Olson, G. H. Thomas, T.-S. Ding, P. C. Rasmussen, R. S. Ridgely, A. J. Stattersfield, P. M. Bennett, I. P. Owens, et al. Global patterns of geographic range size in birds. *PLoS biology*, 4(7):e208, 2006.

J. M. Parody, F. J. Cuthbert, and E. H. Decker. The effect of 50 years of landscape change on species richness and community composition. *Global Ecology and Biogeography*, 10(3):305–313, 2001.

S. Pawar. Community assembly, stability and signatures of dynamical constraints on food web structure. *Journal of theoretical biology*, 259(3):601–612, 2009.

P. Pillai, M. Loreau, and A. Gonzalez. A patch-dynamic framework for food web metacommunities. *Theoretical Ecology*, 3(4): 223–237, 2010.

S. L. Pimm, C. N. Jenkins, R. Abell, T. M. Brooks, J. L. Gittleman, L. N. Joppa, P. H. Raven, C. M. Roberts, and J. O. Sexton. The biodiversity of species and their rates of extinction, distribution, and protection. *Science*, 344(6187):1246752, 2014.

S. J. Plitzko and B. Drossel. The effect of dispersal between patches on the stability of large trophic food webs. *Theoretical Ecology*, 8(2):233–244, 2015.

W. Post and S. Pimm. Community assembly and food web stability. *Mathematical Biosciences*, 64(2):169–192, 1983.

F. W. Preston. The commonness, and rarity, of species. *Ecology*, 29(3):254–283, 1948.

H. R. Pulliam. Sources, sinks, and population regulation. *The American Naturalist*, 132(5):652–661, 1988.

D. L. Rabosky and A. H. Hurlbert. Species richness at continental scales is dominated by ecological limits. *The American Naturalist*, 185(5):572–583, 2015.

T. Reichenbach, M. Mobilia, and E. Frey. Mobility promotes and jeopardizes biodiversity in rock–paper–scissors games. *Nature*, 448(7157):1046, 2007.

R. P. Rohr, S. Saavedra, and J. Bascompte. On the structural stability of mutualistic systems. *Science*, 345(6195):1253497, 2014.

A. Rossberg, A. Caskenette, and L. Bersier. Structural instability of food webs and food-web models and their implications for management. In J. C. Moore, P. C. de Ruiter, K. S. McCann, and V. Wolters, editors, *Adaptive Food Webs: Stability and Transitions of Real and Model Ecosystems*, chapter 22. Cambridge University Press, 2017.

A. G. Rossberg. *Food webs and biodiversity: foundations, models, data.* John Wiley & Sons, 2013.

T. Schoener. The species-area relation within archipelagos: models and evidence from island land birds. In *16th International Ornithological Congress, Canberra, Australia, 12 to 17 August 1974*, pages 629–642. Australian Academy of Sciences, 1976.

A. Shmida and M. V. Wilson. Biological determinants of species diversity. *Journal of biogeography*, pages 1–20, 1985.

N. Takashina, B. Kusumoto, Y. Kubota, and E. P. Economo. A geometric approach to scaling individual distributions to macroecological patterns. *bioRxiv*, 2018. doi: 10.1101/302810.

T. Thiel and B. Drossel. Impact of stochastic migration on species diversity in meta-food webs consisting of several patches. *Journal of theoretical biology*, 443:147–156, 2018.

J. A. Veech. A probability-based analysis of temporal and spatial co-occurrence in grassland birds. *Journal of Biogeography*, 33(12):2145–2153, 2006.

J. A. Veech. A probabilistic model for analysing species co-occurrence. *Global Ecology and Biogeography*, 22(2):252–260, 2013.

M. Vellend, M. Dornelas, L. Baeten, R. Beauséjour, C. D. Brown, P. De Frenne, S. C. Elmendorf, N. J. Gotelli, F. Moyes, I. H. Myers-Smith, et al. Estimates of local biodiversity change over time stand up to scrutiny. *Ecology*, 98(2):583–590, 2017.

A. K. Winegardner, B. K. Jones, I. S. Ng, T. Siqueira, and K. Cottenie. The terminology of metacommunity ecology. *Trends in ecology & evolution*, 27(5):253–254, 2012.

M. S. Wisz, J. Pottier, W. D. Kissling, L. Pellissier, J. Lenoir, C. F. Damgaard, C. F. Dormann, M. C. Forchhammer, J.-A. Grytnes, A. Guisan, et al. The role of biotic interactions in shaping distributions and realised assemblages of species: implications for species distribution modelling. *Biological reviews*, 88(1):15–30, 2013.

H. Xu, M. Detto, S. Fang, Y. Li, R. Zang, and S. Liu. Habitat hotspots of common and rare tropical species along climatic and edaphic gradients. *Journal of Ecology*, 103(5):1325–1333, 2015.

K. Yoshida. Evolutionary dynamics of species diversity in an interaction web system. *Ecological Modelling*, 163(1-2):131–143, 2003.

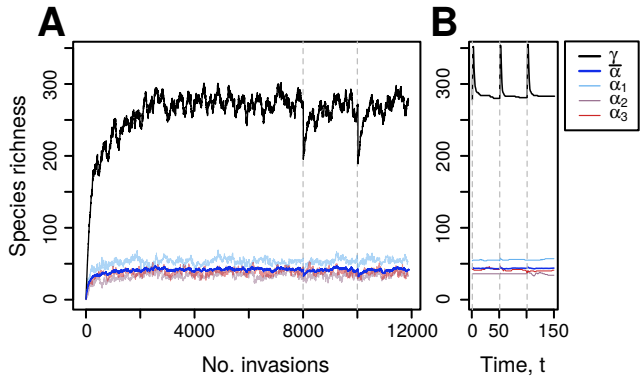

Figure 1: **Biodiversity regulation in model metacommunities.** The emergence of diversity equilibria at multiple spatial scales as a result of a stepwise invasion flux in a typical model metacommunity (A). Regional diversity (γ, black) and the average local diversity ($\bar{\alpha}$, blue) are shown, as well as that observed in three randomly selected patches (α, coloured). Relaxation back to equilibrium following random removal or introduction of large numbers of species (25% of the equilibrium richness, indicated by vertical dashed lines, A and B) reveals the strength and predictability of metacommunity-scale regulation in model assemblages. Relaxation times following removal and introduction differ by several orders of magnitude since the re-accumulation of diversity occurs at the invasion timescale, while extirpations occur at the population-dynamic timescale (measured in units t).

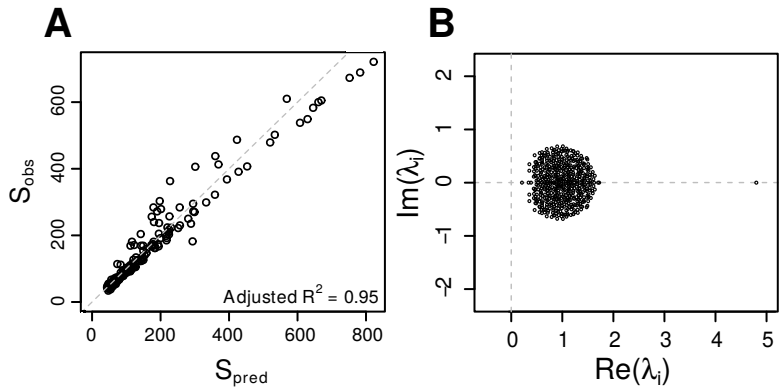

Figure 2: **Testing for biodiversity regulation by structural stability in metacommunity models.** A: Comparison of the regional equilibrium diversity predicted by Eq. 2 and that observed in simulated metacommunities for 195 combinations of patch number and spatial heterogeneity. The dashed line signifies equality. B: The eigenvalue spectrum of a typical regional-scale competitive overlap matrix $\mathbf{C}$. Both analyses strongly suggest the mechanism regulating diversity at the metacommunity scale is the loss of ecological structural stability.

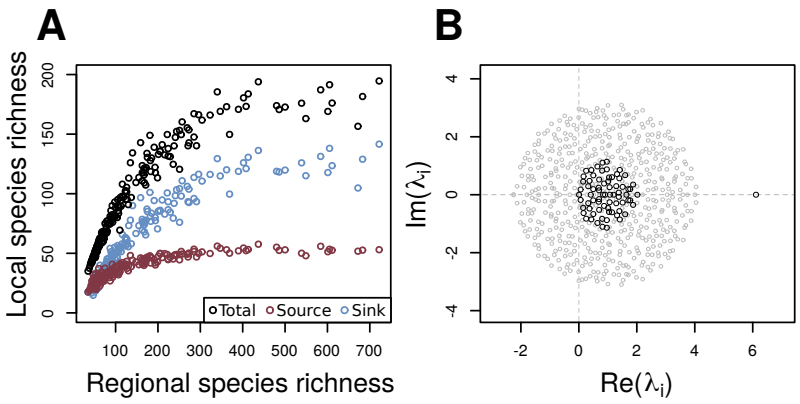

Figure 3: **Demonstration of structurally unstable diversity regulation at the local scale.** A: Average local diversity (black), and that attributed to source (red) and sink (blue) populations, at regional diversity equilibrium, plotted against regional species richness for the same 195 parameter combinations used in Fig. 2. The sublinearity of the local-regional richness relation suggests local communities are saturated with respect to both source and sink diversity for sufficiently high N. B: Comparison of the spectra of the full competitive overlap matrix $\mathbf{A}$ (grey circles) with that of its sub-matrix matrix $\mathbf{A}_{\text{source}}$ (black circles), corresponding to source populations only, for a randomly selected local community at regional diversity equilibrium. The spectrum of $\mathbf{A}_{\text{source}}$ demonstrates the role of structural instability in regulating the diversity of the key, locally sustained component of the local assemblage. The largest eigenvalue of the un-decomposed matrix falls outside of the range shown.

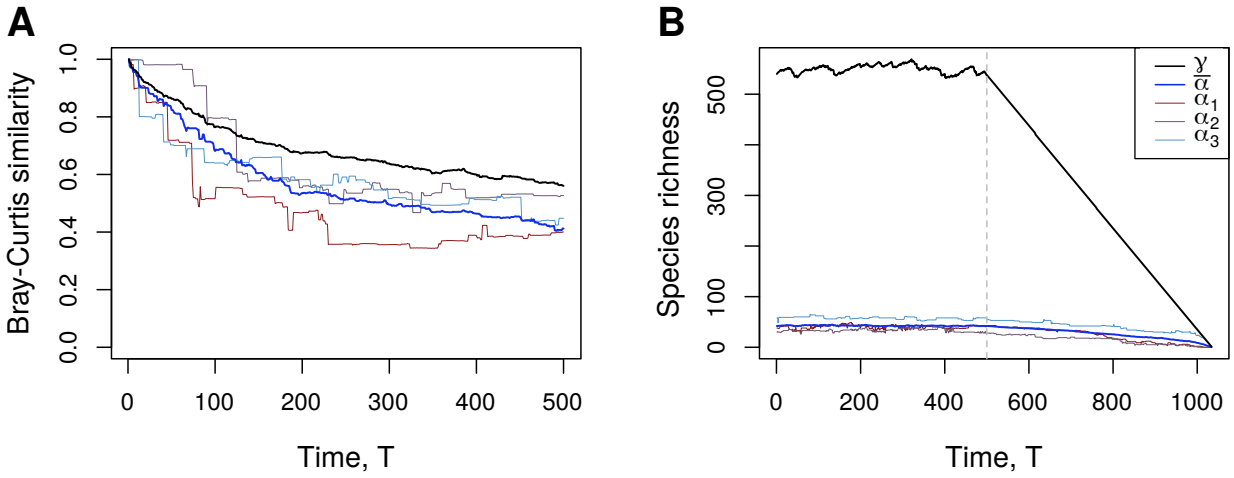

Figure 4: **Temporal trends in community composition and species richness of model communities.** The temporal Bray-Curtis similarity (A) and *source* population species richness (B, $T < 500$) for a metacommunity at regional equilibrium subject to a slow, discrete flux of invaders. Data for the metacommunity (black), the local average (blue) and three randomly selected local communities (coloured) are shown. After 500 invasions the invasion flux in panel (B) is switched off and species are successively removed in order of increasing regional abundance.

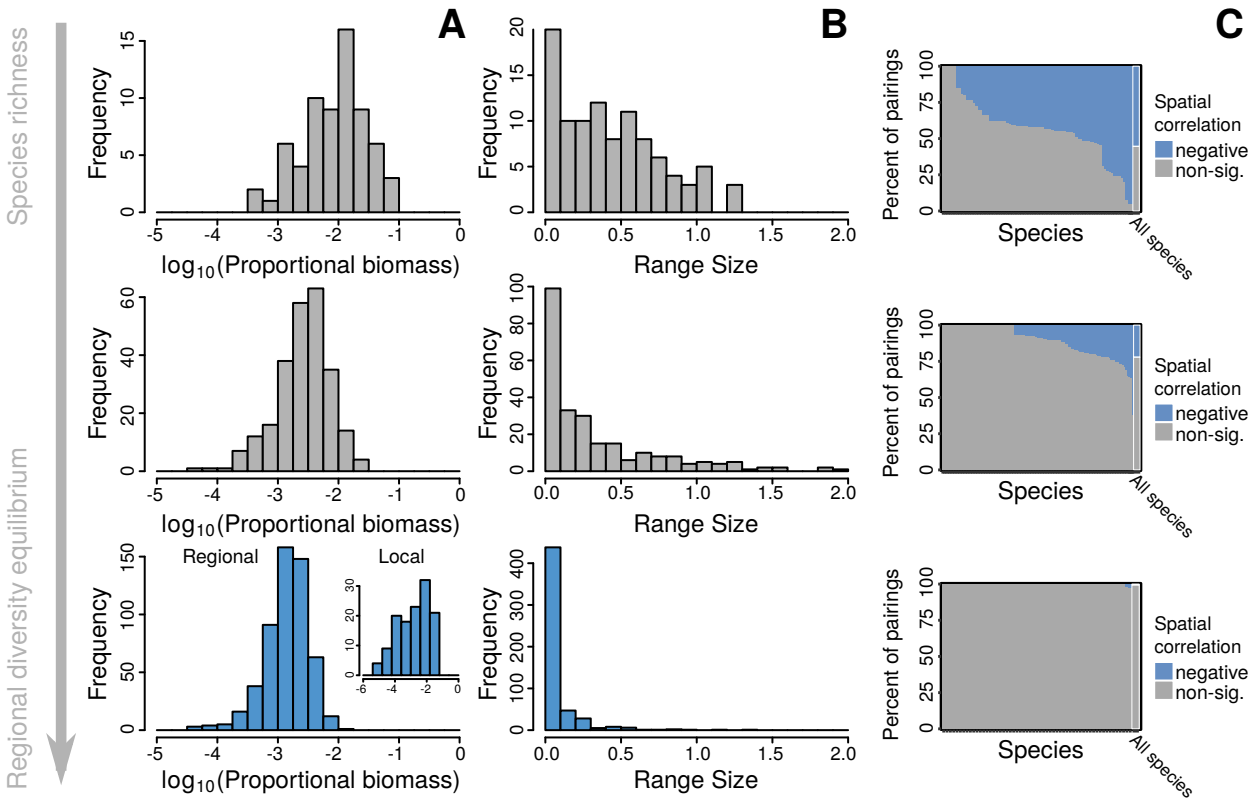

Figure 5: **The effect of regional diversity regulation on macroecology in simulated metacommunities**. Species Biomass Distributions (A), Range Size Distributions (B), and (C) Co-occurrence Profiles (Veech, 2006; Griffith et al., 2016) for a typical model metacommunity at 20, 50, and 100% of the regional diversity equilibrium of around 500 species. In B, an even distribution over the model landscape corresponds to a Range Size measure of 1.7, though for species concentrated near the edges our measure of Range Size can give even larger values. In C, the percentage of possible species pairs that exhibit statistically significant ($p < 0.05$) negative spatial correlation is shown in blue for each species, and for the community as a whole (right-most bar). No significant positive correlations were found. All three distributions converge on patterns well represented in the empirical literature as metacommunities approach the self-organized equilibrium.

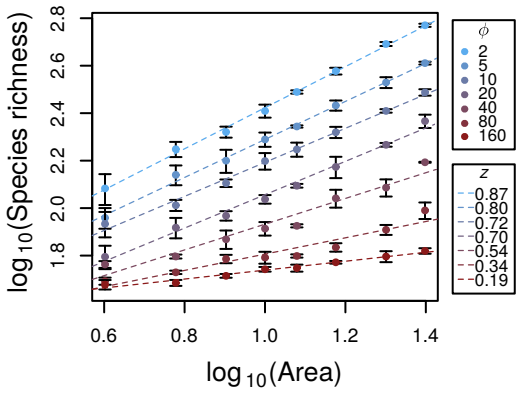

Figure 6: **Species area relations for simulated metacommunities.** Species richness increases as a function of model area according to power laws with exponents ranging from 0.19 to 0.87. Colours indicate the degree of spatial environmental heterogeneity, ϕ. Error bars indicate standard deviations estimated from three independent model runs for each parameterization, for which small differences between simulations arose largely due to the random topography of the model landscapes.

Supporting information

The coupling of local and regional competition coefficients

The interaction between environmental gradients and competitive overlap coefficients in the determination of the regional overlap coefficients $\mathbf{C}_{ij}$ is complex and depends upon the degree of environmental heterogeneity. To test the hypothesis that local interactions ($\mathbf{A}_{ij}$) drive regional community assembly (Rabosky and Hurlbert, 2015) we need to analyse the extent to which fundamental and realised competitive overlap coefficients are correlated. Simple linear regression shos that $\mathbf{A}_{ij}$ and $\mathbf{C}_{ij}$ are indeed significantly correlated ($p < 0.01$, for all parameter combinations), but the strength of the correlation, measured by the adjusted R^2, ranges from 0.1 to 1.0.

Unsurprisingly, given the nature of $\mathbf{C}$, the slope of the relationship $m \leq 1$, with $m \sim 1$ in the homogeneous extreme (high ϕ and/or low N, Fig. S1A), in which case the strength of the correlation between local interactions and regional community assembly is maximised (Fig. S1B). Environmental homogeneity undermines the distinction between adjacent communities and, in the extreme, the idea of a metacommunity.

Spatial structure at the metapopulation scale

The combined effect of local and regional diversity regulation drives spatial turnover in community composition. Species in model metacommunities near regional limits converge on highly aggregated spatial distributions in which biomass decays exponentially as a function of distance from regional maxima (Fig. S2, note the logarithmic colour gradient).

Regional scale competitive overlap matrices

Fig. S3A-B highlights the difference in magnitude of the regional scale interaction coefficients, which incorporate the complex spatial coexistence mechanisms active in heterogeneous landscapes. Spatial coexistence mechanisms in model metacommuities can be understood as slowing the onset of structural instability by modifying the distribution in competitive overlap coefficients. The spectrum of the 'microcosmic' competitive overlap matrix $\mathbf{A}$ (Fig. S3C), fully covering the origin of the complex plane, highlights the fact that such an assemblage would be biologically unfeasible in the absence of the abiotic (topographical and environmental) variation in the model.

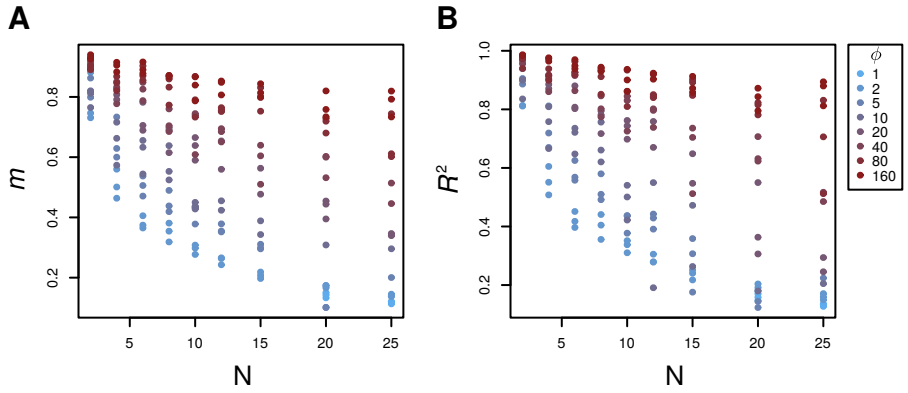

Figure S1: **The statistical relationship between interspecific competitive overlap coefficients $\mathbf{A}_{ij}$ and $\mathbf{C}_{ij}$.** The slope of the linear regression of the elements of $\mathbf{C}_{ij}$ against those of $\mathbf{A}_{ij}$ (A) and the adjusted R^2 of the relationship (B). Colours code spatial environmental heterogeneity, ϕ.

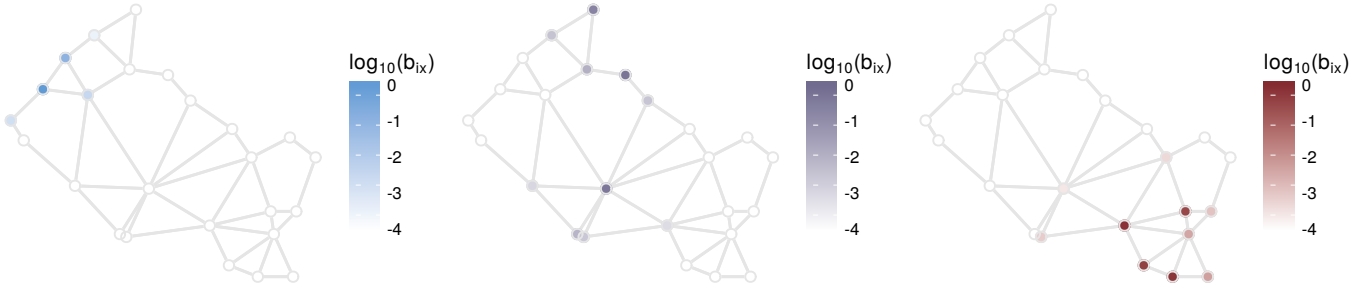

Figure S2: **A typical spatial model landscape and the distribution of biomass for three simulated species.** Dispersal corridors (gray links) in random spatial networks were assigning using the Gabriel Algorithm. Colours correspond to three randomly selected species biomass distributions. Spatial aggregation is a key characteristic of species ranges in strongly regulated metacommunities.

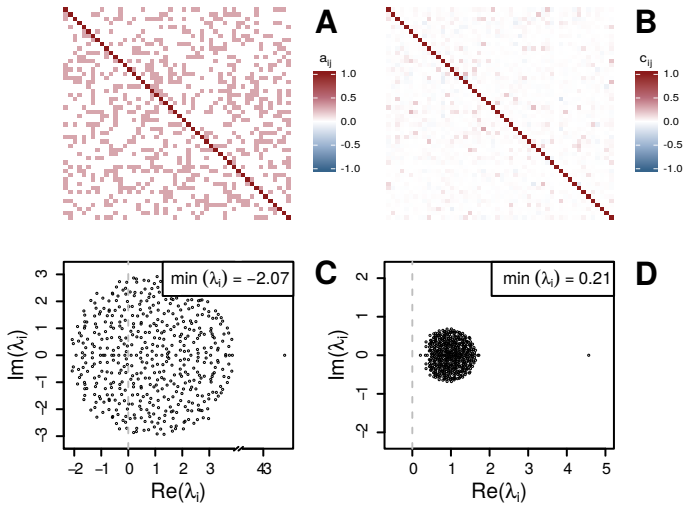

Figure S3: **Comparison of the matrices A and C for a single metacommunity at regional diversity equilibrium.** The local competitive overlap matrix **A** (A) and regional *effective* competitive overlap matrix **C** (B) for a randomly sampled subset (for visual clarity) of a typical model metacommunity ($N = 20$, $\phi = 1$) at regional diversity equilibrium and the corresponding eigenvalue spectra (C and D). The off-diagonal elements, $\mathbf{C}_{ij}$, incorporate the effects of both spatial segregation and 'indirect mutualism' (which can lead to negative values). The spectrum of the regional overlap matrix **C**, which approaches the origin as diversity saturates, matches that observed in spatially unresolved models (Rossberg, 2013).